World Academy of Science, Engineering and Technology
International Journal of Environmental and Ecological Engineering
Vol:11, No:5, 2017

Preparation of Sorbent Materials for the Removal of Hardness and Organic Pollutants from Water and Wastewater

Thanaa Abdel Moghny, Mohamed Keshawy, Mahmoud Fathy, Abdul-Raheim M. Abdul-Raheim, Khalid I. Kabel, Ahmed F. El-Kafrawy, Mahmoud Ahmed Mousa, Ahmed E. Awadallah

***Abstract*—**Ecological pollution is of great concern for human health and the environment. Numerous organic and inorganic pollutants usually discharged into the water caused carcinogenic or toxic effect for human and different life form. In this respect, this work aims to treat water contaminated by organic and inorganic waste using sorbent based on polystyrene. Therefore, two different series of adsorbent material were prepared; the first one included the preparation of polymeric sorbent from the reaction of styrene acrylate ester and alkyl acrylate. The second series involved syntheses of composite ion exchange resins of waste polystyrene and amorphous carbon thin film (WPS/ACTF) by solvent evaporation using micro emulsion polymerization. The produced ACTF/WPS nanocomposite was sulfonated to produce cation exchange resins ACTF/WPSS nanocomposite. The sorbents of the first series were characterized using FTIR, ^{1}H NMR, and gel permeation chromatography. The thermal properties of the cross-linked sorbents were investigated using thermogravimetric analysis, and the morphology was characterized by scanning electron microscope (SEM). The removal of organic pollutant was determined through absorption tests in a various organic solvent. The chemical and crystalline structure of nanocomposite of second series has been proven by studies of FTIR spectrum, X-rays, thermal analysis, SEM and TEM analysis to study morphology of resins and ACTF that assembled with polystyrene chain. It is found that the composite resins ACTF/WPSS are thermally stable and show higher chemical stability than ion exchange WPSS resins. The composite resin was evaluated for calcium hardness removal. The result is evident that the ACTF/WPSS composite has more prominent inorganic pollutant removal than WPSS resin. So, we recommend the using of nanocomposite resin as new potential applications for water treatment process.

***Keywords*—**Nanocomposite, sorbent materials, waste water, waste polystyrene.

I. Introduction

WATER hardness is the major amount of calcium and magnesium cations in water. The hardness in water is naturally occurring in groundwater, and also, it is present locally from industrial effluent such as chemical and mining industry or the excessive use of lime to this oil in agriculture field. From the other view, there is a serious threat to rivers, marine environment, and human life due to petroleum oils which contain various petroleum products such as polycyclic aromatic hydrocarbons (PAHs), which in turn induce carcinogenic and immune toxic effects as well as endocrine disruption in vertebrates. Because oil leakage causes large water polluted area in a short time, it should be removed from water surface as soon as possible to protect the oceanic environment and livings [1], [2]. There are different ways to clean up water from oil pollution, such as mechanical collections, in situ burning, and using of the absorbent materials. In addition, the hardness removal includes ion exchange resins and other methods. Absorbent materials find applications in collection and complete removal of spilled oil, and thus, they help in preventing environmental pollution. One application of ion-exchange resins is using it to remove poisonous and heavy metal ions from polluted water by exchanging them with relatively safer ions, such as sodium, hydrogen, and potassium ions [3]-[5].

Polystyrene is an inexpensive and hard plastic; it is produced by free radical vinyl polymerization of styrene. A large portion of polystyrene's production goes into packaging (cups, plates, bowls, trays, clamshells, meat trays, yogurt and cottage cheese containers) and protective packaging (shaped and pieces used to ship electronic goods such as audio/visual cassettes). There are some methods for recycling polystyrene waste including chemical and thermal recycling. Accordingly, we look forward to synthesizing two series of adsorbent materials based on chloromethyl styrene (CMS) as a monomer and WPS [6]-[9].

In this work, styrene and WPS were used to prepare two sorbent groups used as oregano gel and cation exchange resin, respectively. In the first series, styrene was copolymerized with 4-chloromethyl styrene, and the poly (styrene-co-4-chloromethyl styrene) ester (PSCMS) that was produced was reacted with acrylic acid to produce macromonomer containing polymerizable C=C (St-CMS acrylate) which subsequently copolymerized with acrylate in presence of crosslinker to obtain the crosslinked copolymers (organo gel). In the second series, the composite ion exchange resins of waste polystyrene and amorphous carbon thin film (WPS/ACTF) was prepared. In this respect, a waste polystyrene sulfonate (WPSS)/resin was prepared from reaction of styrene polymer (polystyrene) with sulfuric acid, then the ACTF was

Thanaa Abdel Moghny is with the Petroleum Application Department, Egyptian Petroleum Research Institute, Cairo11727, Egypt (e-mail: Thanaa_h@yahoo.com).

Mohamed Keshawy, Mahmoud Fathy, Abdul-Raheim M. Abdul-Raheim, Khalid I. Kabel and Ahmed E. Awadallah are with the Petroleum Application Department, Egyptian Petroleum Research Institute, Cairo11727, Egypt.

Ahmed F. El-Kafrawy is with the Faculty of Science, Ain Shams University, Cairo11727, Egypt.

Mahmoud Ahmed Mousa is with the 3Faculty of the Science Benha University, Fred NadaStreet, Banha-Cairo, Egypt.

suspended and folded by waste polystyrene sulfonate (WPSS) to produce ACTF/WPSS hybrid nanocomposite. The prepared compounds were characterized by different physicochemical tools and evaluated for removal of organic pollutant and hardness, respectively.

II. Experimental

A. Materials

Styrene (vinylbenzene, Aldrich, 99%) and p-chloromethylstyrene (4-Vinylbenzyl chloride, Aldrich, 90%) were distilled from stabilizer. Divinyl benzene (DVB) and benzoyl peroxide (BPO) were recrystallized from a methanol solution. Acrylic acid (Aldrich), triethyl amine (TEA), ethylhexyl acrylate (EHA), methylene bisacrylamide (MBA), methylene chloride and methanol were used as received. To measure the swelling capacities of the prepared gels, we use toluene, chloroform, N,N-dimethyl formamide (DMF), petroleum diesel (PD). The inorganic chemicals including $CaCI_2$ $2H_2O$, HCI, and NaOH were obtained from Merck (Darmstadt, Germany) in analytical grade. All solutions were prepared using distilled water.

B. Cobalt Silicate Nanoparticles Preparation

4.0 g of cobalt silicate was stirred vigorously for 30 minutes at 45 °C in ethanol solution of 200 ml until the suspend emulsion formed. The powder was collected and drying at 50 °C for 8h in a vacuum oven [4], [9].

C. Amorphous Carbon Thin Film (ACTF) Preparation

Rice straw was subjected to pretreatment process using 1% (wt./wt.) sulphuric acid for 60 minutes at 120 ºC. The lignin was delignificated at 1200 ºC for 60 minutes using a mixture of 1.5% (wt./wt.) NaOH and 0.5% (wt./wt.) H_2O_2. The amorphous carbon thin film (ACTF) was prepared from cellulose produced from lignification of rice straw as illustrated in [4], [9].

D. Preparation of Self-Assembled (ACTF) /WPS Hybrid Nanocomposite

Self-assembled (ACTF/WPS) hybrid nanocomposite was prepared as indicating in reference 40 ºC [4], [9].

E. Sulfonation of Ion-Exchange Resin

20.4 g of WPS and ACTF/WPS were put in a bottom glass flask reactor (500 cm^3) equipped with mechanical agitation, vertical condenser, and thermometer. The flask containing the solution was heated in the silicone oil bath to 48-52 °C in the presence of sulfating agent acetyl sulfate to produce WPSS and ACTF/WPSS. Then, the ACTF/WPSS and WPSS resins wre isolated and dried in oven for 24h at 30 °C [10], [11].

F. Synthesis of Poly (Styrene-co-p-Chloromethyl Styrene) Ester (PSCMS)

In 100-ml three-necked flask, styrene and p-chloromethyl styrene monomers (3.12 g and 1.5 g, respectively), 0.02 wt.% of BPO were dissolved in 15mL toluene, then the mixture was stirred under N_2 atmosphere at 60 ºC for 12h to obtain the desired copolymer (PSCMS). The solution was cooled and precipitated in methanol and dried under vacuum. 1 g of PSCMS was dissolved in 50 mL of DMF at room temperature and poured in a 250 ml three-necked flask, then 7 g of TEA was added, and the solution was cooled to 0 ºC. After that, 5 g of acrylic acid was added dropwise, and the reactant solution was stirred at 60 ºC for 12h. Such mixture was precipitated by methanol and washed with water, then dried at 40 ºC for 24h. [7].

G. Synthesis of Cross-Linked Copolymer

Copolymerization and crosslinking of PSCMS ester and ethylhexyl acrylates (EHA) was performed through coagulation followed by bulk polymerization. The acrylate ester monomer was dissolved in mixture solvent of methylene chloride and methanol (9:1 by volume) and mixed together with (EHA) in presence of 0.04 wt.% benzoyl peroxide (BPO) free radical initiator. Then, different weight ratios of DVB or MBA crosslinker ranging from 1-6% (w/w) were mixed and bubbled with nitrogen. The copolymerization reactions were performed in siliconized test tubes at 72 ºC for 12h. The previous step was repeated at different (mol% PSCMS ester/mol% EHA) ratios to prepare different compositions of oil sobers.

H. Characterization of the Prepared Compounds

The chemical structures of the produced copolymers were confirmed by using FTIR (Nicolet IS-10 FT-IR) and1HNMR spectroscopy (300 M.Hs. Spectrophotometer W–P-300, Bruker) in DMSO as a solvent. Thermal properties of the prepared copolymers were determined using TGA: Q 600 SDT simultaneous DSC-TGA, the samples were heated from 25 °C to 600 °C in N_2 flow (20 cm min^{-1}) at a heating rate 10 °C/min. Finally, the morphology of the prepared copolymers was characterized by SEM, Jeol, Model JSM5300 at 15 keV.

I. Effect of Contact Time

The equilibrium of contact time was measured for 5.0 g resin solubilized in 100 ml synthetic hard water solution at 200 rpm in pH range between 2.0 and 5.0 for 60 minutes [12].

J. Effect of pH

The sorption of Ca (II) ions and removal of hardness from hard water solution were studied with the WPSS and ACTF/WPSS at initial pH ranges between 2.0 and 5.0. The initial pH of hard water solution was controlled by adding hydrochloric acid and sodium hydroxide solutions at 298 K and 200 rpm for 60 minutes [12].

K. Effect of Resin Weight

The efficiency of WPSS and ACTF/WPSS resins to adsorb calcium ions from aqueous media was studied at the adjusted pH of 7.0±0.1, and resin dosage was set between 0.025 to 0.350 g [12].

L. Extraction of Soluble Fraction

Soluble fraction (SF) can be extracted from gel fraction by weighing known quantity of gel after drying in dichloromethane (DCM) solvent and washing three times at room temperature over a 24h period. After that, the swelled

polymer was dried in a vacuum at room temperature for 48h. The SF was expressed as the fractional loss in weight of cross-linked zero gel [13], [14] and calculated according the following equation:

$$SF\ \% = ((W0 - W)/ W0)\ X\ 100)$$

where W0 and W are the weight of the polymers before and after extraction with DCM, respectively.

M. Determination of Oil Absorption Capacity of the Prepared Organo-Gels

The oil absorption capacity was determined by a weighing method according to ASTM (F726-81): a measured amount of gels placed in a stainless-steel mesh having dimensions of 4x4x2 cm. Then, this mesh with the gels had been immersed in different organic solvents (DMF, toluene, chloroform, and petroleum diesel) and weighed beforehand. The oil sample was collected and withdrew for 30 second, where the excess oil was tapped with filter paper and then weighed. The swelling capacity (Q) was determined by weighing the swelled gel and calculated from the following equations:

$$Q\ (g/g) = \frac{(\text{weight of swollen gel} - \text{weight of dried sample})}{\text{weight of dried sample}}$$

III. Results and Discussions

A. Structure Confirmation by FTIR

The characteristic FT-IR spectrum of PSCMS in Fig. 1 (a) presented peaks at 3025 (str. C-H aromatic), 2922 and 2850 cm^{-1} (str. C-H aliphatic), 1490 and 1600 cm^{-1} (str. C=C aromatic), 678 cm^{-1} (C-Cl stretching vibration). On the other hand, FT-IR spectrum of PSSMA copolymer in Fig. 1 (b) showed the weakening of the band at 678 cm^{-1}(C-Cl stretching vibration) and the appearance of strong bands at 1722 and 1148 cm^{-1} which represents C=O & C-O stretching of ester group, respectively. FTIR data showed that the reaction between PSCMS and acrylic acid was successfully completed [15].

FTIR data showed that the reaction between of ACTF/WPS in Fig. 2 displayed the bands at 697, 1449, and 1491 cm^{-1} for the mono substituted aromatic ring of polystyrene/amorphous carbon, also a vibration band appears at 1027 cm^{-1} [21]. Furthermore, a broad band appeared at 3460 cm^{-1} for OH group which may drift to lower frequency due to interaction of hydrogen bond in water molecule and oxygen atom in the amorphous carbon [12]. On the other hand, the FTIR spectra of ACTF/WPS in Fig. 2 displayed the bands at 697, 1449, and 1491 cm^{-1} for the mono substituted aromatic ring of polystyrene/amorphous carbon [13].

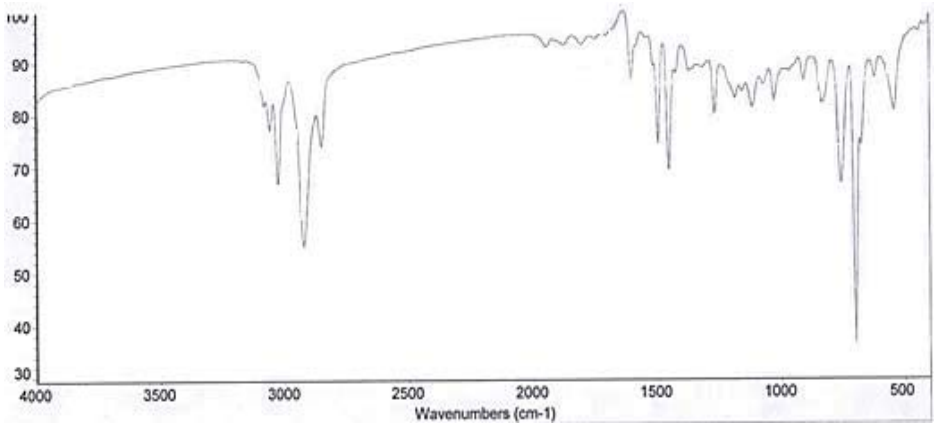

(a)

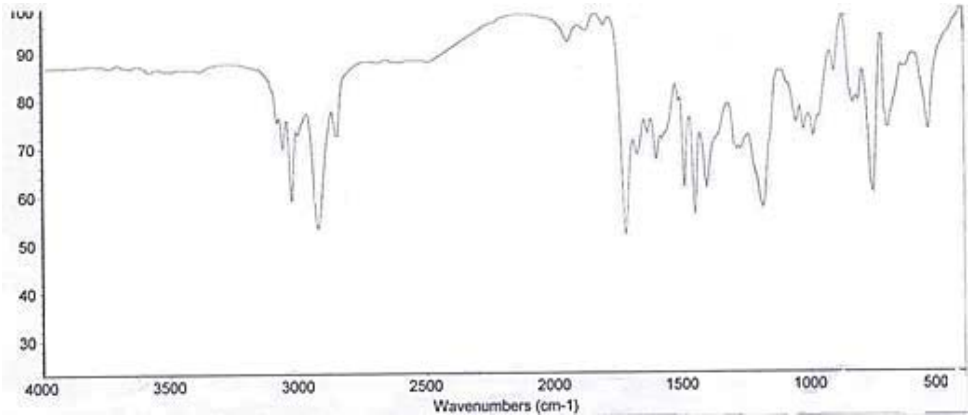

(b)

Fig. 1 FTIR for (a) PSCMS and (b) PSSMA ester

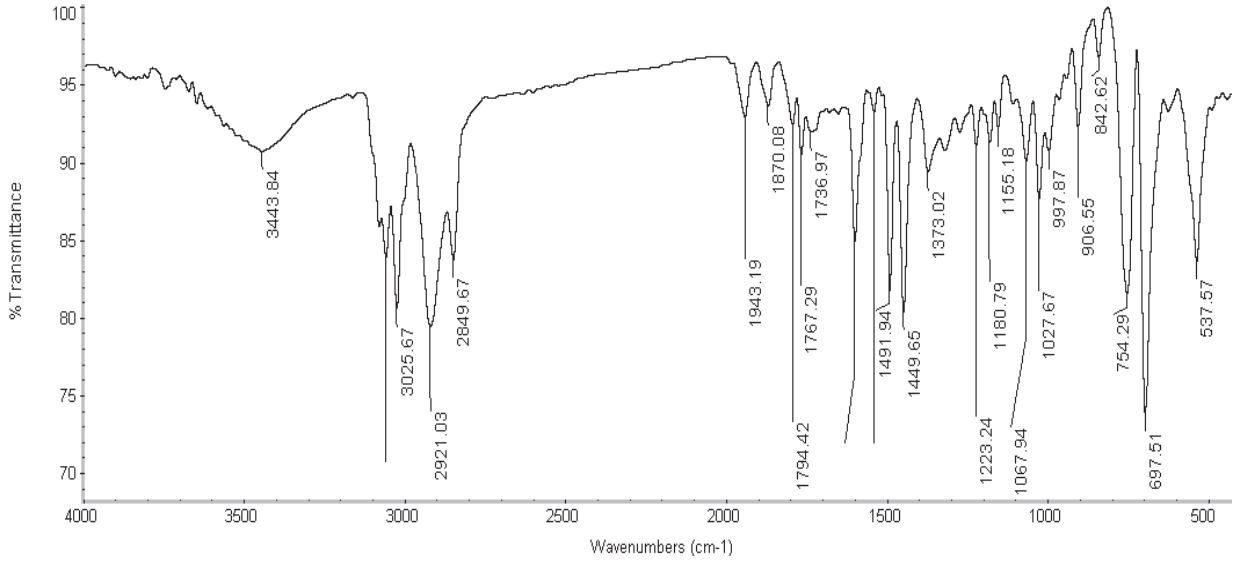

Fig. 2 FTIR analysis of amorphous carbon film/waste polystyrene resin

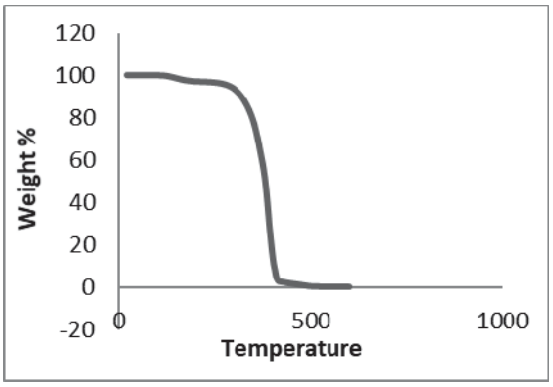

Fig. 3 TGA analysis of amorphous carbon film/waste polystyrene resin

B. Thermal Analysis

The thermal analysis of ACTF/WPS resin presented in Fig. 3 shows the presence of three main weight loss peaks, one at low temperature due to loss of residual ethanol, water, toluene and/or the sulfonic groups, the second step ongoing at 200 °C and finishing at 400 °C [16], this means a complete thermal decomposition. The thermal stabilities of (ACTF/WPS) resin exhibited an increase in thermal stability of composite polymer as compared with the corresponding waste polystyrene.

The thermal properties of the prepared copolymers were studied after extraction of SF. There is no any weight loss which appears below 100 °C in TGA plots, indicating that no water or ethanol was retained in copolymer. TGA showed that the oil gels had a good thermal stability due to its thermal decomposition temperature appeared over 300 °C as shown in Figs. 4 and 5. These figures show two degradation steps; the first one may be attributed to decomposition of EHA that has a short hydrocarbon chain length and ester linkage with low thermal stability, the second one due to decomposition of PSSMA having aromatic rings with high thermal stability. Accordingly, the thermal stability of crosslinked copolymer increases with increasing the molar ratio of PSSMA.

In general, the crosslinking increases the thermal stability of a polymer and the change in glass temperature (Tg) depends upon the crosslinking degree [17]. The effect of crosslinker concentration on the thermal stability was shown in Fig. 4 for (PSSMA/EHA 50/50) at different DVB%, it is found that the decomposition temperature observed at 207 and 233 °C corresponding to 10% weight loss, whereas the decomposition temperature at 50% weight loss occurred at 400 and 430 °C, for 1 and 6% DVB, respectively. This means that, with increasing the crosslinker concentration from 1 to 6%, the thermal stability of cross-linked copolymers increases due to increase of crosslinking densities in cross-linked copolymers.

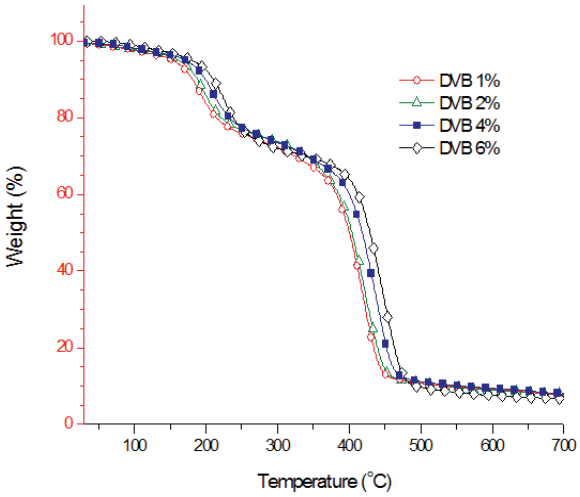

Fig. 4 Thermogravimetric analysis for PSSMA/EHA 50/50 molar ratio at different DVB concentrations

On the other hand, the effect of molar ratio on the thermal stability was proven in Fig. 5, and TGA curves of PSSMA/EHA show successive increasing in the thermal stability with increasing PSSMA concentration and decreasing

acrylate (EHA) concentration. The decomposition temperature was observed at 200, 240, and 370 °C for copolymers PSSMA/EHA 10/90, PSSMA/EHA 50/50 and PSSMA/EHA 90/10, respectively corresponding to 10% weight loss, whereas 50% weight loss takes place at 390, 415, and 437 °C for the same copolymers, respectively.

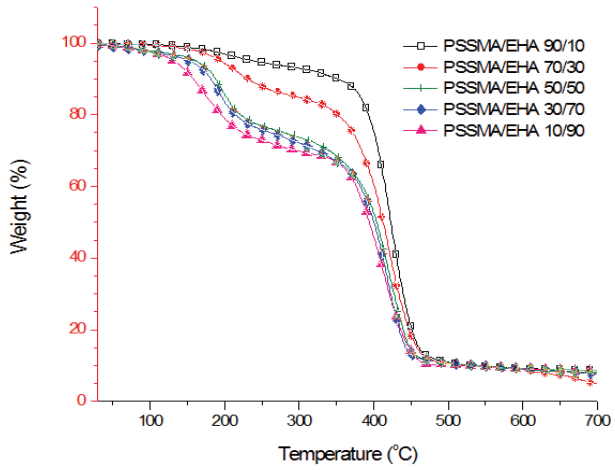

Fig. 5 Thermogravimetric analysis for PSSMA/EHA different molar ratio at DVB

C. SEM Analysis

The morphology of PSCMS ester/EHA copolymer was examined to study the effect of copolymer composition and crosslinker concentration on the porosity of copoloymers networks. The SEM microphotographs of crosslinked copolymers were displayed in Figs. 6 and 7. It is apparent that there were many small random pores in the crosslinked copolymers; these pores will support large surfaces in the polymeric network. The morphology of a crosslinked resins will influence the rate of oil sorbed [18]. All SEM photographs show skin layer structure and possess homogenous wall-like texture. Hence, Fig. 6 (a) (PSSMA/EHA 90/10) shows a smooth flat surface with some cracks. With increasing the EHA content, we noticed the appearance of random pores in Fig. 6 (b) (PSCMS/EHA 50/50). But, after excessive increase of EHA, the surface seems to be rougher fractured and random pores become smaller Fig. 6 (c) (PSCMS/EHA 10/90). Meanwhile, the gels (50/50) are better absorbents for most of the organic solvents than the others. SEM photographs in Fig. 7 display the effect of cross-linker concentration on the morphology of (PSCMS/EHA 50/50) copolymer at different DVB concentrations. Fig. 7 (a) reveals large pores at 2% DVB, and by increasing the cross-linker concentration, the pores become smaller (Fig. 7 (b)) due to increase the crosslink density, and hence, decreasing the oil swelling capacity [19]-[21].

SEM analysis in Fig. 8 shows the penetrated of ACTF inside the composite polystyrene, and the WPS polymer chain is folded the amorphous carbon film. This can be explained by non-covalently bond between WPS and ACTF, which in turn affected the thermal stability of prepared nanocomposite. The top left areas in Fig. 8 show the emerging of carbon film inside the resin and covered for all aspects, and this shows the compatibility between polymers and nano amorphous carbon film.

D. Contact Time

Through the contact time study, we found that the resins prepared by the new sulfonation process have very high adsorption susceptibility toward the calcium ion as shown in Fig. 9, hence the dynamic stage starts after 20 minutes, and the dynamic exchange occurs between ions in the solution and resins [22].

E. Effect of pH

It is clear from Fig. 10 that highest adsorption of calcium ion values occurs in the basic media because there is an abundance of hydrogen ions in solution, which is considered as competitive ion with calcium ion. Moreover, the lowest ion exchange value attained at 300 mg /L, whereas the ion-exchange value in the neutral pH media lies between 300-450 mg /L and reaches to the highest value in the basic media at 500 mg/L. Through these pH results, one can conclude that the rank of cationic exchange column can be laid before anion exchange resin in case of brackish water soften [23].

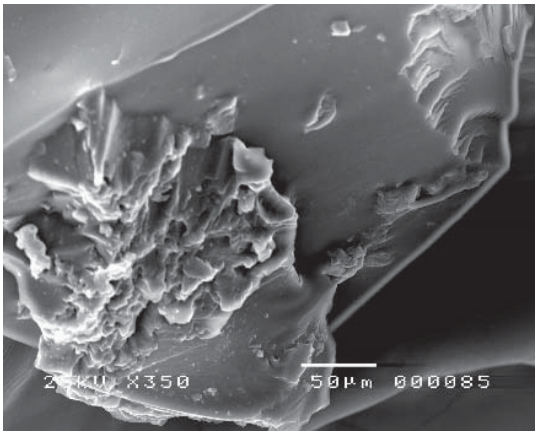

(a) 90/10

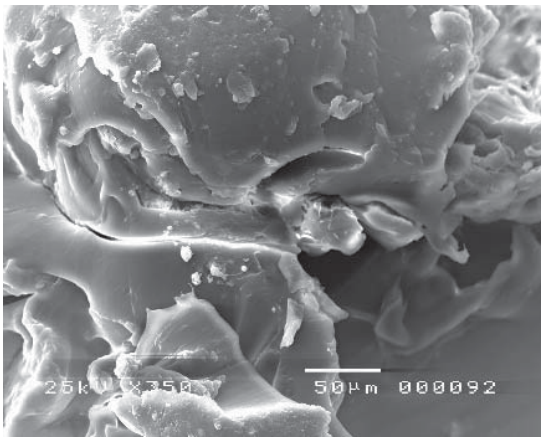

(b) 50/50

Fig. 6 SEM images of PSSMA/EHA 2% MBA a) 90/10 & b) 50/50

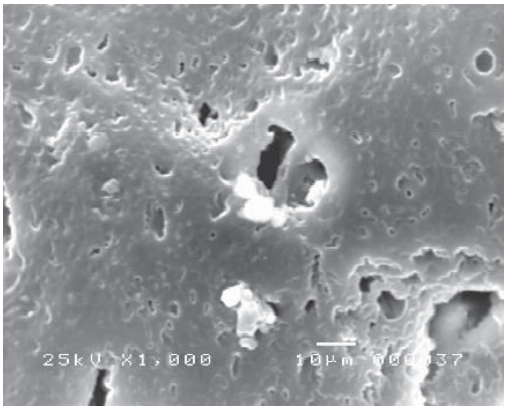

(a) DVB 2%

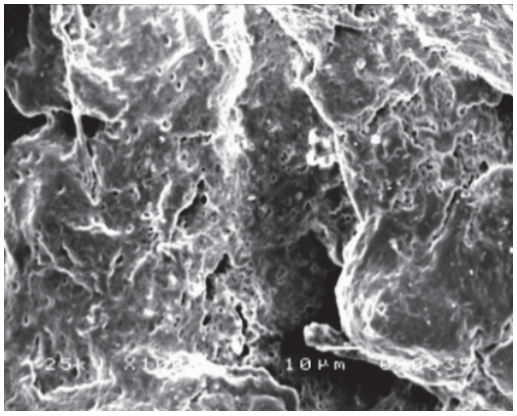

(b) DVB 6%

Fig. 7 SEM images of PSSMA/EHA: 50/50 a) 2% DVB & b) 6% DVB

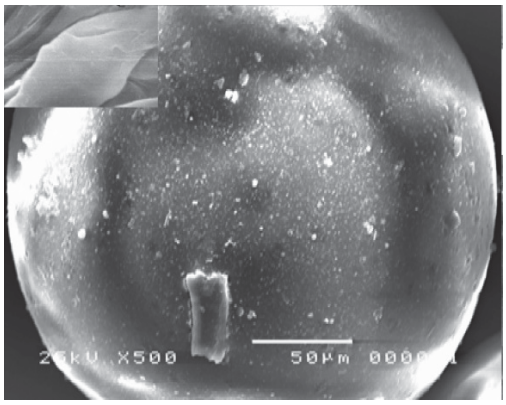

Fig. 8 SEM analysis of amorphous carbon film/waste polystyrene resin

F. Effect of Resin Dosage

It is seen from Fig. 11 that the prepared resins have the ability to remove the calcium ions by 98% at neutral pH at 0.2 mg of resins because active site was saturated [23].

G. Effect of Cross-Linked Type and Content on Oil Absorbency

Chemical crosslinking, meaning the formation of short sequences of chemical bonds or covalent bonds joining two polymeric chains with each other, is also responsible for the formation of three-dimensional network structures that characterize the oil sorbent material [13]. Accordingly, the percentage of cross linker in our copolymerization system was investigated to study the relationship between swelling capacity and the concentration of DVB or MBA cross linkers, therefore a series of poly (PSCMS/EHA) 50/50 mol% with varied DVB or MBA content (from 1 to 6 wt.%) were prepared. For brevity, the swelling results in DMF were presented in Figs. 12 (a) and (b) for DVB and MBA.

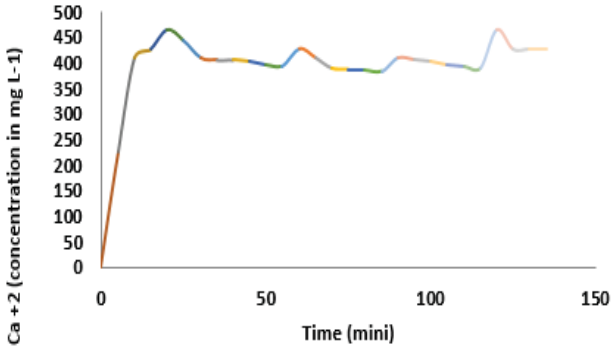

Fig. 9 Effect of contact time between resin and synthetic solution of hard water on removal of hardness of calcium

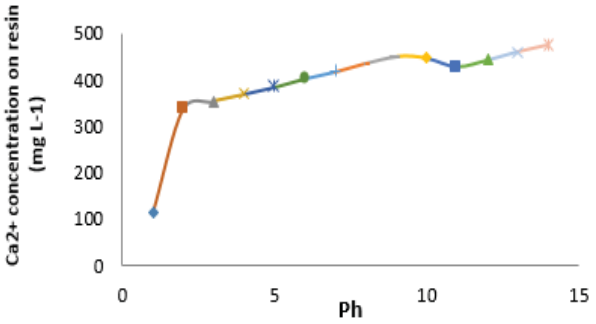

Fig. 10 Effect of pH on Removal of Hardness of Calcium

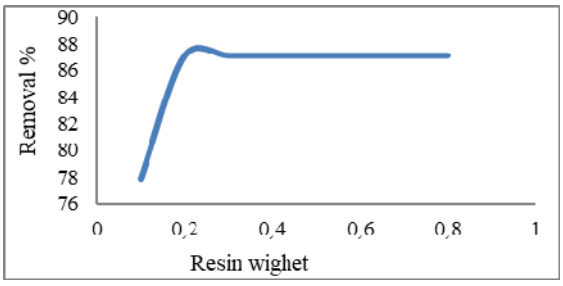

Fig. 11 The effect of resin dosage on the exchange of calcium ion by sulfonated waste polystyrene resin

It was found that, with increasing the DVB or MBA%, the oil absorbency of cross-linked PSCMS/EHA increased at first, reached a maximum, and then decreased. This decrease may be due to restricted relaxation of polymeric chain. At (1 wt.%) DVB cross linker, the PSCMS/EHA, containing many soluble materials (SFs) such as, linear polymers and polymer chains which are insufficiently cross-linked, the crosslinking density

in the cross-linked copolymers was decreased, which in turn resulted to lower Q max (maximum oil absorbency) to 71.3 g/g. On contrary, at higher DVB% (6 wt.%) the Qmax becomes 69.3 g/g, which means formation of too dense cross-linked network, and subsequently, it decreased the oil absorbency. Thus, 2 wt.% is an appropriate DVB content to provide Qmax of 82.7 g/goil absorbency, while 4 wt.% of MBA gives an appropriate Qmax of 43.5 g/gas illustrated in Figs. 12 (a) and (b), respectively. We also noticed that oil absorbency in case of DVB cross linker is higher than that of MBA at the same concentration and the same solvent. This can be attributed to the reactivity of DVB towards crosslinking.

H. Effect of Molar Ratio on Oil Absorbency

We have studied the effect of monomer feed ratio on oil absorbency at fixed cross linker type, concentration and fixed solvent. For this purpose, the effect of PSCMS and EHA molar ratio on oil absorbency for DMF, $CHCl_3$, toluene, and diesel solvents is shown in Figs. 13 (a) and (b) for 2%DVB and 4%MBA, respectively at PSCMS/EHA monomer feed ratios of 90/10, 70/30, 50/50, 30/70, and 10/90. It is reported that the concentration of acrylate has an effect on the hydrophobicity, the crosslinking density of the cross-linked copolymers, and the glass transition temperature [24]. For all PSCMS/EHA cross-linked copolymers, oil absorbency increased by increasing the EHA concentration due to the increase in hydrophobicity. Fig. 13 (a) illustrated the effect of molar ratio on oil absorbency in case of 2% DVB cross linker, e.g. the Qmax of (PSCMS/EHA 90/10) in DMF recorded at 66.5 g/g, and it increased to 82.6 g/g with increasing EHA molar ratio to (PSCMS/EHA 50/50) and then decreased and reaches its lower value to 35.6 g/g with increasing EHA concentration over 50 mol% at (PSSMACMS/EHA 10/90). This attributed to decrease crosslinking density with increasing the EHA concentration, because the reactivity of styrene acrylate toward DVB is higher than that of EHA toward DVB, and the oil absorbency was increased. However, a further increase in EHA monomer feed ratio over 50 mol%, the weight% of the EHA molar ratio, promotes the side reaction of EHA, which leads to increase the crosslinking density, and thus, relatively slow increase in oil absorbency. In case of MBA cross linker (Fig. 13 (b)), the Qmax started at 47.9 g/g for (PSCMS/EHA 90/10) and increases as EHA concentration increases to reach its higher value 65.3 g/gat (PSCMS/EHA 70/30) and finally decreases to become 28.5 g/g at PSSMA/EHA 10/90.

It is reported that petroleum absorptivity depends on bulkiness and length of alkyl substituent and especially on porosity of the microstructure. It has been established that hydrophobicity and the effective volume of the crosslinking network are affected by monomer feed ratio [25], [26].

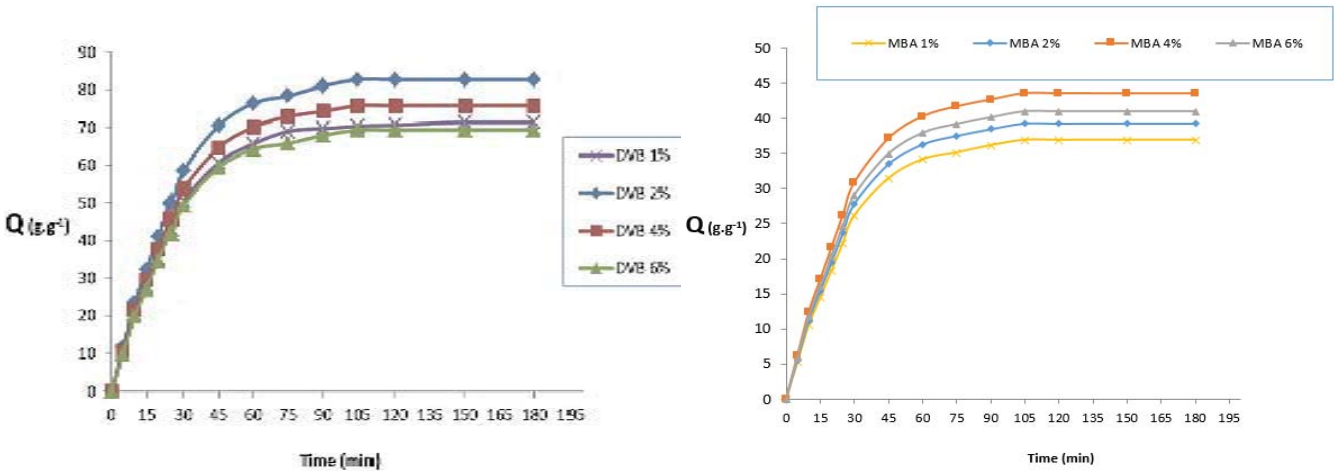

(a) (b)

Fig. 12 Swelling of PSSMA/EHA (50/50 molar ratio) in DMF (a) at different DVB (crosslinker) content (b) at different MBA (crosslinker) content

IV. Conclusion

High oil absorbents (PSCMS/EHA) were successfully prepared through free radical polymerization from styrene acrylate and EHA in presence of either DVB or MBA as crosslinker and BPO as initiator. The thermal stability of organogel was investigated; the prepared gels were thermally stable. The morphology of oil sorbent was also studied, and the gel had a smooth flat surface with some cracks. In addition, the SFs of oil sorbent was decreased with increasing the crosslinker concentration and decreasing the acrylate content. Moreover, the effects of reaction conditions, such as crosslinker type and content, molar ratio were studied. It is found that the oil absorbency increased with increasing the acrylate (EHA) molar ratios and decreasing the amount of crosslinker and reached its maximum when the amount of crosslinker is 2 wt.% in case of DVB and (4 wt.%) in case of MBA. Finally, the organogel attains the maximum swelling capacity during 1.5h, and the high oil sorption capacity makes it an attractive sorbent for oil spill cleanup.

In this study, the matrix of waste polystyrene will be sulfonated by acetyl sulfate reagent, then resin was used by adding ACTF to remove the calcium ions from brackish water. It is found that the interaction between the amorphous carbon films and WPS causes a reinforcement effect since the amorphous carbon films improved the thermal properties of the prepared nanocomposite resin, thereby, ion-exchange capacity of waste polystyrene resin and calcium removal were improved. We found that the prepared resins can remove the calcium ions by 98% at neutral pH at 0.2 mg of resins. Therefore, it is advised to use such resins for desalination of brackish water from calcium ion.

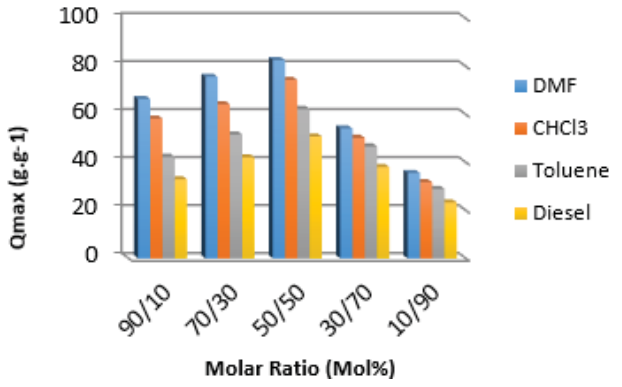

(a)

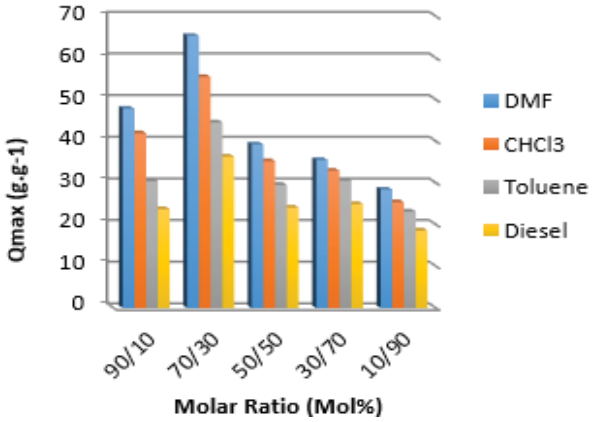

(b)

Fig. 13 Swelling of PSSMA/EHA at different molar ratio in DMF, $CHCl_3$, Toluene and Diesel for a) at 2%DVB b) at 4% MBA (crosslinker)

REFERENCES

[1] K, B., S. R and K. N (2016). "Exploration of microporous bio-carbon scaffold for efficient utilization of sulfur in lithium-sulfur system." Electrochimica Acta 209: 171-182.

[2] Jouhara, H., V. Anastasov and I. Khamis (2009). "Potential of heat pipe technology in nuclear seawater desalination." Desalination 249(3): 1055-1061.

[3] Abbas, A. (2006). "Model predictive control of a reverse osmosis desalination unit." Desalination 194(1–3): 268-280.

[4] Fathy, M., T. A. Moghny, M. A. Mousa, A.-H. A.-A. El-Bellihi and A. E. Awadallah (2016). "Synthesis of Transparent Amorphous Carbon Thin Films from Cellulose Powder in Rice Straw." Arabian Journal for Science and Engineering: 1-9.

[5] Mestre, A. S., A. Nabiço, P. L. Figueiredo, M. L. Pinto, M. S. C. S. Santos and I. M. Fonseca (2016). "Enhanced clofibric acid removal by activated carbons: Water hardness as a key parameter." Chemical Engineering Journal 286: 538-548.

[6] Gao, H., Z. Song, W. Zhang, X. Yang, X. Wang and D. Wang "Synthesis of highly effective absorbents with waste quenching blast furnace slag to remove Methyl Orange from aqueous solution." Journal of Environmental Sciences.

[7] Mallakpour, S. and E. Khadem (2016). "Carbon nanotube–metal oxide nanocomposites: Fabrication, properties and applications." Chemical Engineering Journal 302: 344-367.

[8] Mondal, S., K. Aikat and G. Halder (2016). "Biosorptive uptake of ibuprofen by chemically modified Parthenium hysterophorus derived biochar: Equilibrium, kinetics, thermodynamics and modeling." Ecological Engineering 92: 158-172.

[9] Fathy, M., T. Abdel Moghny, M. A. Mousa, A.-H. A.-A. El-Bellihi and A. E. Awadallah (2016). "Absorption of calcium ions on oxidized graphene sheets and study its dynamic behavior by kinetic and isothermal models." Applied Nanoscience: 1-13.

[10] An, Z., H. Zhang, Q. Wen, Z. Chen and M. Du (2014). "Desalination combined with copper (II) removal in a novel microbial desalination cell." Desalination 346: 115-121.

[11] Ataollahi, N., K. Vezzù, G. Nawn, G. Pace, G. Cavinato, F. Girardi, P. Scardi, V. Di Noto and R. Di Maggio (2017). "A Polyketone-based Anion Exchange Membrane for Electrochemical Applications: Synthesis and Characterization." Electrochimica Acta 226: 148-157.

[12] Venugopal, K. and S. Dharmalingam (2014). "Evaluation of synthetic salt water desalination by using a functionalized polysulfone based bipolar membrane electrodialysis cell." Desalination 344: 189-197.

[13] Abdel-Azim Abdel-Azim, A., Abdul-Raheim, A. M., Atta Ayman, M., Brostow, W., &Datashvili, T. (2009) e-Polymers, 9:pp.1592.

[14] Masqué, N., Galia, M., Marcé, R., & Borrull, F. (1998) J. Chromatogr. A, 803: 147-155.

[15] Yan, W., L. Wang, C. Chen, D. Zhang, A.-J. Li, Z. Yao and L.-Y. Shi (2016). "Polystyrene Microspheres-Templated Nitrogen-Doped Graphene Hollow Spheres as Metal-Free Catalyst for Oxygen Reduction Reaction." Electrochimica Acta 188: 230-239.

[16] Lim, G.-T., H.-G. Jeong, I.-S. Hwang, D.-H. Kim, N. Park and J. Cho (2009). "Fabrication of a silica ceramic membrane using the aerosol flame deposition method for pretreatment focusing on particle control during desalination." Desalination 238(1–3): 53-59.

[17] Jang, J., & Kim, B.-S. (2000) J. Appl. Polym. Sci., 77: 903-913.

[18] Zhou, M. H., & Cho, W. J. (2003) J. Appl. Polym. Sci., 89: 1818-1824.

[19] Rastegarpanah, A. and H. R. Mortaheb (2016). "Surface treatment of polyethersulfone membranes for applying in desalination by direct contact membrane distillation." Desalination 377: 99-107.

[20] Sabir, A., A. Islam, M. Shafiq, A. Shafeeq, M. T. Z. Butt, N. M. Ahmad, K. Sanaullah and T. Jamil (2015). "Novel polymer matrix composite membrane doped with fumed silica particles for reverse osmosis desalination." Desalination 368: 159-170.

[21] Kumar, R., A. F. Ismail, M. A. Kassim and A. M. Isloor (2013). "Modification of PSf/PIAM membrane for improved desalination applications using Chitosan coagulation media." Desalination 317: 108-115.

[22] Saleh, T. A., A. M. Muhammad and S. A. Ali (2016). "Synthesis of hydrophobic cross-linked polyzwitterionic acid for simultaneous sorption of Eriochrome black T and chromium ions from binary hazardous waters." Journal of Colloid and Interface Science 468: 324-333.

[23] Misra, B. M. (2007). "Seawater desalination using nuclear heat/electricity- Prospects and challenges." Desalination 205(1–3): 269-278

[24] Jang, J., & Kim, B.-S. (2000) J. Appl. Polym. Sci., 77: 914-920.

[25] Coday, B. D., L. Miller-Robbie, E. G. Beaudry, J. Munakata-Marr and T. Y. Cath (2015). "Life cycle and economic assessments of engineered osmosis and osmotic dilution for desalination of Haynesville shale pit water." Desalination 369: 188-200.

[26] El-Manharawy, S. and A. Hafez (2003). "A new chemical classification system of natural waters for desalination and other industrial uses." Desalination 156(1–3): 163-180.